Performance Study of Mixed Flow Impeller by Means of Partial Impellers

Tatsuo Kawada, Yoichiro Matsumoto, Hideo Ohashi
Department of Mechanical Engineering, University of Tokyo
and
Kazuhiro Tanaka
Department of Mechanical Engineering, Sophia University

1. INTRODUCTION

Mixed flow impellers are widely used for fans, compressors and pumps, owing to their adaptability for a broad range of specific speed, filling the gap between axial and centrifugal impellers. As the interest in energy saving becomes acute, mixed flow impellers have attracted substantial attention because of their favourable performance especially at off-design conditions. The present study was conducted as a part of a joint research project managed by JSME under the title "Application of quasi-three dimensional analysis to the design of high performance mixed flow turbomachinery" [1].

In the design of an impeller of a turbomachine, the concept of specific speed plays an important role. The optimum meridional shape of an impeller and its performance characteristics are almost prescribed by its specific speed, if we follow the conventional design practice. The past efforts have been concentrated on the accumulation of such correlation data between performance and specific speed.

There arises, however, a question to this practice. Let us consider two impellers, a prototype and its partial impellers with a reduced, say a half, discharge. Partial impellers can be produced by cutting off the tip section of original blades, so that the passage area is also reduced to the half of the original one. If the viscous effect of passage walls, i.e. hub and casing, is negligible, the discharge and shaft power of the partial impeller at design condition must reduce to the half but the pressure rise may remain unchanged, since the flow in the partial impeller is merely a fraction of the original one. In this case the reduction of specific speed to $1/\sqrt{2}$ of the original value results in no change in the characteristics and the meaning of specific speed as a design parameter will disappear.

The above mentioned situation has reality, only when the viscous effect on the flow is non-existent. By viewing this situation from the opposite standpoint, the viscous effect on the performance can be separately extracted by comparing the characteristics of partial impellers with each other.

The basic motive of the present study lies in this idea.

As the prototype of this study, a mixed flow impeller with a medium specific speed is selected. Three partial impellers are reproduced from the prototype and the performance tests are conducted for these four impellers. After comparing the measured characteristics from various viewpoints, discussions are made for the influence of viscosity on the performance.

2. TEST IMPELLERS AND PERFORMANCE TEST RIG

As the prototype of the present study, a mixed flow open impeller with a medium specific speed, n_s=750 in m^3/min, m, rpm or type number k=1.8, installed in a casing of nearly 30 degree cone angle is selected. This can be considered as typical and representative of mixed flow impellers with quite a broad variation. Principal design specifications of this impeller are listed in Table 1. The geometries of the prototype is determined by a conventional design procedure based on the assumed slip factor [2] and circular arc blade generation on each stream surface. Seven three dimensional blades are mounted on a conical hub of 50 degree cone angle. This prototype is denoted hereafter as Impeller A.

Quasi-three dimensional potential flow analysis [3,4] is applied to this impeller and meridional stream lines as well as pressure distributions along rotating blades are determined. Three meridional stream lines between hub and casing contours, which divide total flow rate Q into four equivalent parts at design flow rate, are then determined as shown in Fig. 1. These stream lines constitute casing contours of three partial Impellers B, C, and D with design flow rate of 3Q/4, 2Q/4 and Q/4, respectively. Along with the prototype impeller of flow rate Q, four impellers in total are tested for the performance comparison.

As far as inviscid potential flow is concerned, these four impellers have completely the same flow at design condition, since the flow in each impeller is merely a fraction of the same solution. The performance of these impellers must be identical, if the viscous effect is non-existent. Test impellers are made of transparent acrylic resin, so that the velocity distribution in the rotating blade passages can be

TABLE 1. Principal specifications

Design capacity	Q_d=0.309	m^3/s
Design total pressure	P_t=121	Pa
Rotational speed	n =1000	rpm
Specific speed	n_s=750	m^3/min m rpm
Impeller outerdiameter	D =350	mm
Peripheral speed	u_2=18.3	m/s
Number of blades	7	
Hub angle	50° (conical hub)	

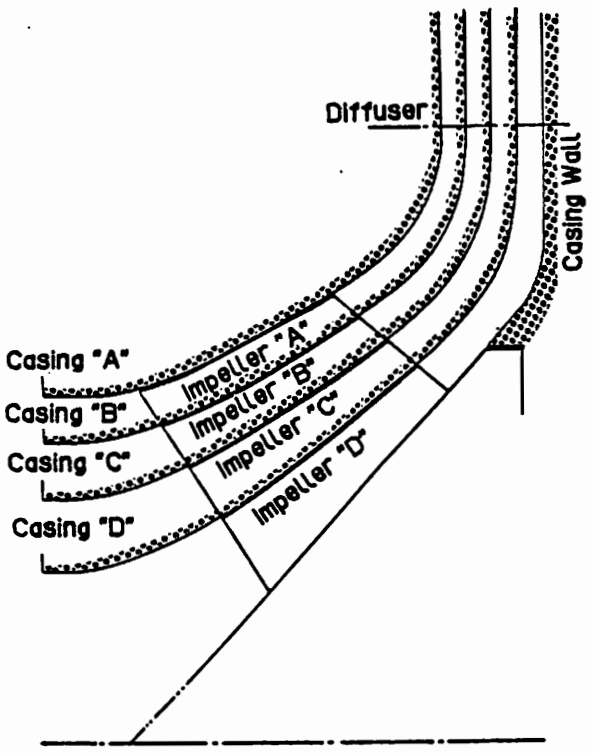

FIGURE 1. Partial impellers

measured by LDV. The tip clearance of all impellers are adjusted to 0.5 mm to the curved casing. The maximum rotational speed of the impellers is around 1000 rpm, limited mainly by the strength of plastic material.

The performance test is carried in air and the test rig is illustrated in Fig. 2. Air is sucked through a suction pipe, whose inner diameter coincides with the inlet eye diameter of individual impeller. The discharge from the test impeller is guided to a parallel walled radial vaneless diffuser

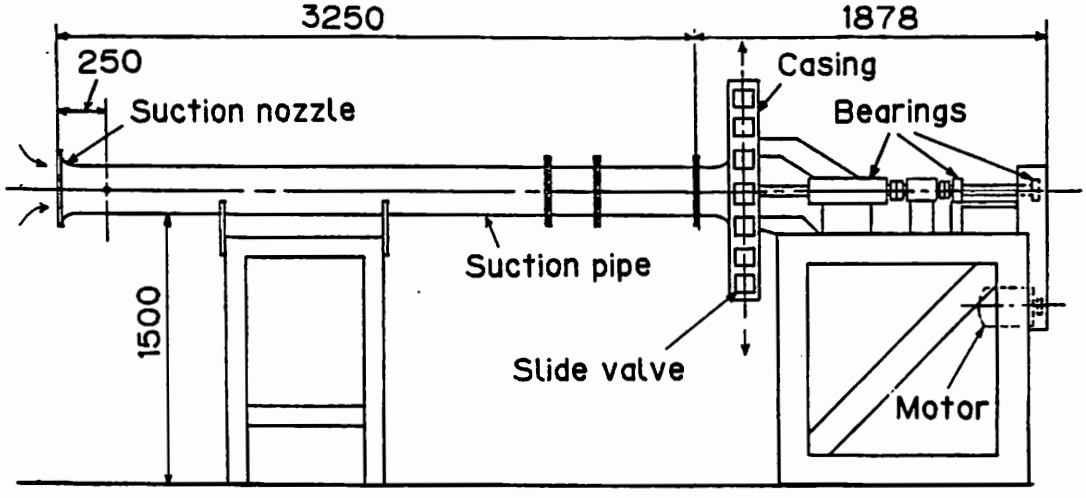

FIGURE 2. Performance test rig

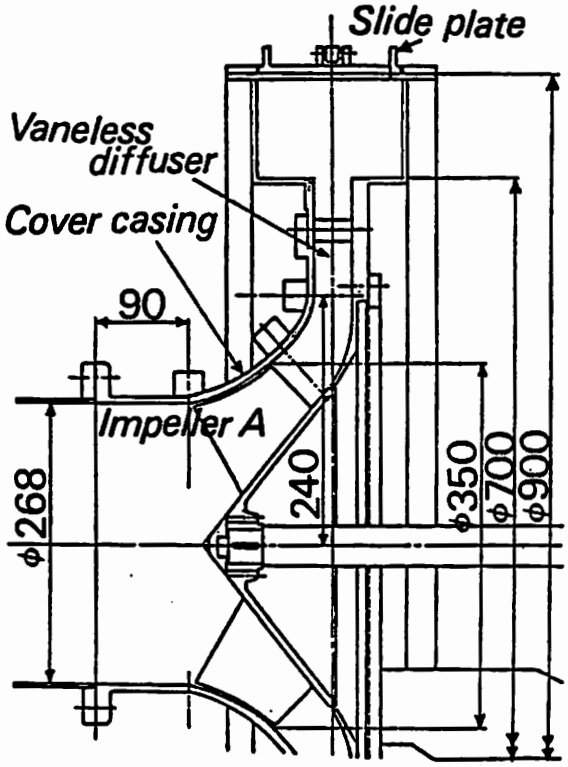

FIGURE 3. Detailed configurations of the impeller passage: Impeller A.

with passage width proportional to its design flow rate as shown in Fig. 3. The discharge is controlled by throttling the slide valve arranged at the periphery of the radial diffuser.

3. MEASUREMENT

Flow rate is calculated from the pressure drop at the suction nozzle attached at the inlet of the suction pipe. The discharge total pressure of the impeller is measured at traverse section 3 indicated in Fig. 4. Measurements are made by cobra type three-hole yawmeter at the center of five equally divided flow passages and the mass-flow weighted average of these five data are adopted as discharge total pressure.

The total inlet pressure is defined at inlet section 0 as the sum of wall pressure and dynamic pressure calculated from mean velocity in the suction pipe. Meridional velocity and flow angle are also measured at immediately up- and downstream of the impeller (traverse section 1 and 2) and at the discharge section 3. The total pressure rise is calculated as the difference of discharge and inlet total pressure and thus is affected only by losses in the impeller, excluding all other losses in diffuser and suction pipe.

Special attention is paid to evaluate net driving power of

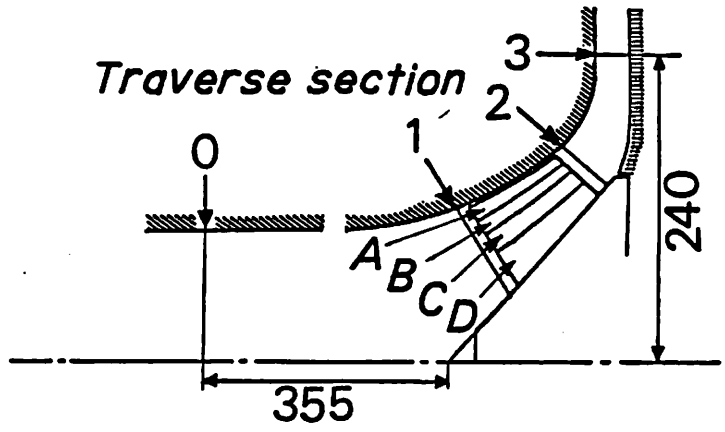

FIGURE 4. Location of measurement pressure distribution

the impeller, because the impeller power and bearing losses are almost comparable in this experiment. To exclude bearing losses, the impeller hub is directly attached to the rotating shaft end via load cells and the signals are transmitted to stationary amplifiers through slip rings. The output of load cells is calibrated by applying static loads before and after every set of measurement and the conversion factors are determined by the method of least squares.

4. DEFINITION OF NON-DIMENSIONAL PARAMETERS

Measured performances are converted to non-dimensional parameters such as flow coefficient ϕ , pressure rise coefficient ψ , power coefficient τ and efficiency η . Two kinds of normalization are introduced as follows; one to describe the characteristics of individual impeller independently and the other to compare the individual characteristics with those of the prototype.

4.1 Normalized by the Quantities of Individual Impeller

Flow coefficient; $\phi = Q/(Au_2)$

Pressure rise coefficient; $\psi = \Delta P_t / \{(1/2)\rho u_2^2\}$ (1)

Power coefficient; $\tau = L/\{(1/2)\rho A u_2^3\}$

where $A = \pi d^2/4$ and $u_2 = \pi dn$ (see NOMENCLATURE for other quantities). Here the outer diameter of each impeller d is used as the representative length.

4.2 Normalized by Referring to the Prototype

According to the non-viscous theory, the performance of a partial impeller must coincide with those of the prototype, if the flow rate is multiplied by the factor given in Table 2. Therefore, the characteristics expressed by the following non-dimensional parameters must be also identical at

TABLE 2. Multiplication factor i

Impeller	A	B	C	D
Factor i	1	4/3	2	4

least at design condition. Deviation of these characteristics can be understood as the influence of viscous effect.

Flow coefficient; $\phi_0 = Q \cdot i/(A_0 u_0)$

Pressure rise coefficient; $\psi_0 = \Delta P_t/\{(1/2)\rho u_0^2\}$

Power coefficient; $\tau_0 = L \cdot i/\{(1/2)\rho A_0 u_0^3\}$ (2)

Efficiency; $\eta = \phi_0 \cdot \psi_0/\tau_0$

where $A_0 = \pi D^2/4$ and $u_0 = \pi Dn$. Outer diameter of prototype impeller D is used as the representative length for all impellers.

In order to extract the characteristics of impeller blades, excluding losses associated with the friction of rotating hub, following power coefficient and efficiency are further introduced.

$$\tau_b = \frac{\text{(input power to impeller)-(input power to dummy rotor)}}{(1/2)\rho A_0 u_0^3} \times i$$

$$\eta_b = \phi_0 \cdot \psi_0/\tau_b \quad (3)$$

Dummy rotor consists of only hub portion without blades.

5. TEST RESULTS

5.1 Velocity Distribution Immediately Up- and Downstream of Impeller

At traverse section 1 immediately upstream of impeller inlet, a reversed flow region is observed near the blade tip at partial flow rate for Impeller A and B, but not for Impeller C and D with narrower passage width. Fig. 5 (a), (b) and (c) show the meridional velocity distributions at traverse section 2 immediately downstream of impeller exit for Impeller A, B and D. As seen from the figures (a) and (c), the tendency of distribution for Impeller A and B becomes quite opposite when flow rate reduces to its minimum. This is due to the development of large reversed flow regions at the inlet tip and exit hub, which result in a strong radial deflection of the flow similar to the one in a centrifugal impeller.

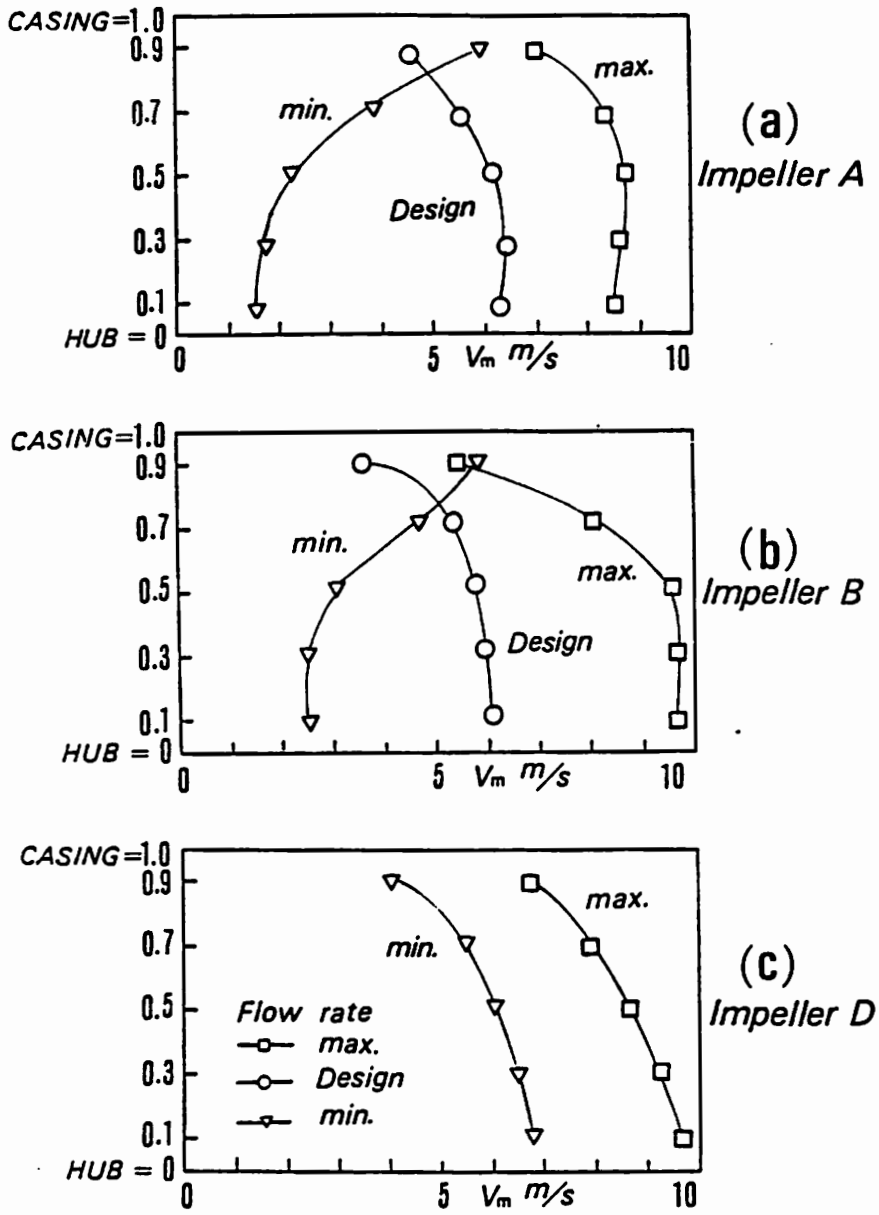

FIGURE 5. Meridional velocity distributions

In Impeller D with the narrowest passage width, radial deflection at partial discharge is restricted by casing and hub walls and the velocity distribution keeps a similar tendency over entire flow rate.

5.2 Shaft Power

Shaft powers of Impeller A - D are plotted in Fig. 6 against flow rate, where that of dummy rotor at zero flow rate is also indicated for comparison. As the passage width of impellers decreases, the maximum flow rate and power input decrease accordingly.

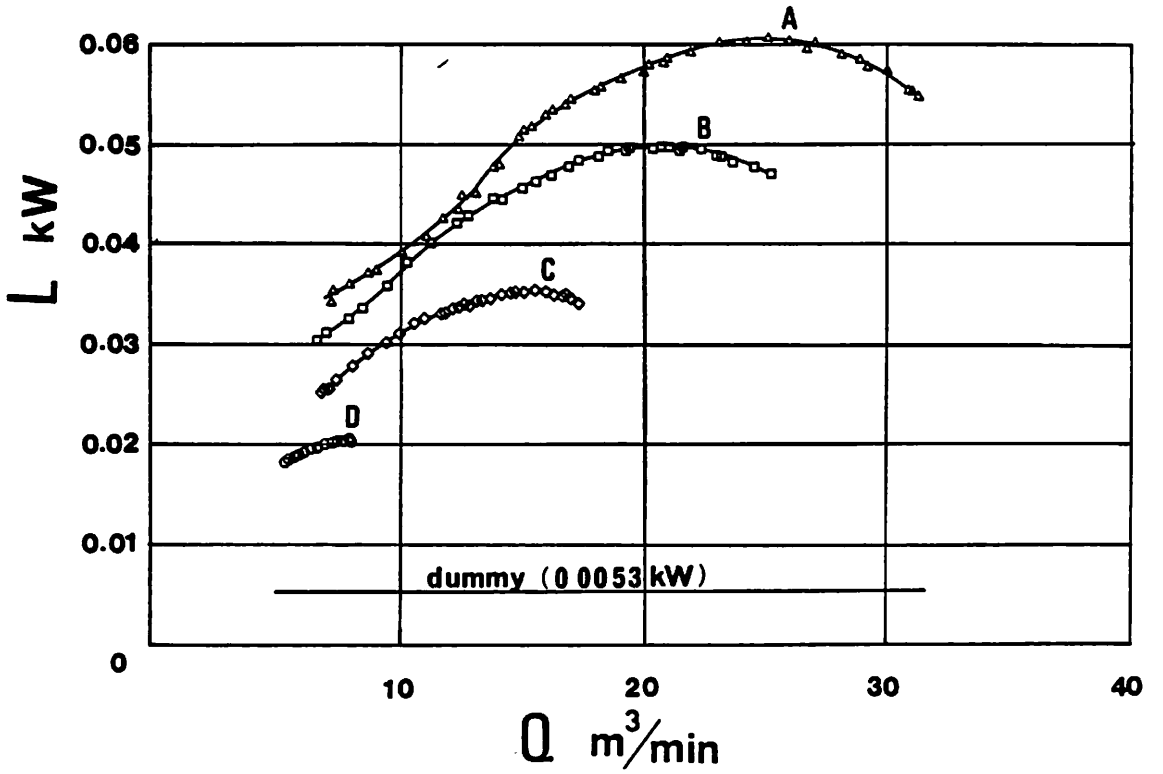

FIGURE 6. Shaft power

5.3 Characteristics of Individual Impellers

Fig. 7 (a) to (d) show the characteristics of individual Impellers A to D using non-dimensional parameters defined by Eq.(1). Pressure rise of every impeller exceeds the design value by a large margin. The reason consists in that the assumed design efficiency η=0.75 was too low as impeller efficiency excluding diffuser losses.

The performance and specific speed of individual impellers at the best efficiency point are listed in Table 3.

TABLE 3. Performance and specific speed at best efficiency point

Impeller	Capacity Q (m^3/min)	Total pressure P_t (Pa)	Power L (kW)	Maximum efficiency η_{max}	Specific speed n_s (m^3/min, m, rpm)
A	24.0	134.1	60.7	0.884	718
B	17.8	135.2	48.1	0.835	614
C	13.3	127.2	34.0	0.830	556
D	6.4	123.7	19.4	0.684	394

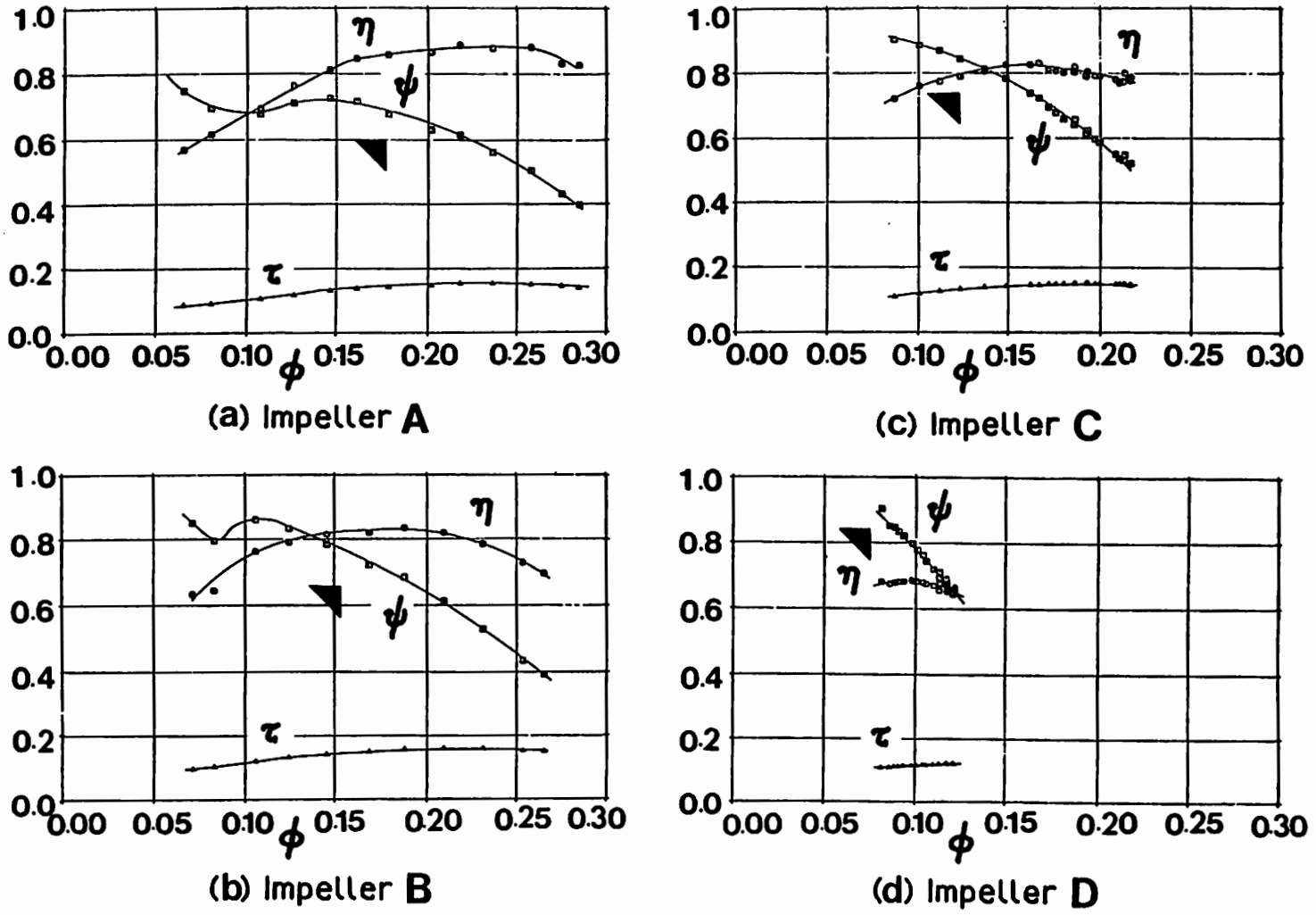

FIGURE 7. Characteristics of individual partial impeller: ◥ shows the design point.

5.4 Comparison of Characteristics Referred to the Prototype

Flow rate versus pressure rise. Fig. 8 (a) shows the relation between flow and pressure rise coefficients defined by Eq.(2) for Impeller A to D. As stated already, these characteristics curves must coincide each other, if the real flow in each impeller is close to the one calculated by potential flow analysis and the efficiency of each impeller is at the same level.

As clearly seen from the figure, the characteristics of four tested impellers coincide almost perfectly at design condition (ϕ_0=0.175). This implies that the flow in each impeller is very close to the calculated one and the fluid dynamic losses due to wall friction at hub and casing surfaces and to blade drag are not much different.

The above conclusion is only true near design condition. The disagreement of characteristics curves becomes obvious at partial and over-flow region, where flow field becomes highly three dimensional due to enhanced secondary flow and developed separation. The wider the passage width (Impeller D to A), the stronger the influence of such three dimensional behavior and hence the bigger the deviation of real flow from the one predicted by potential flow theory.

Flow rate versus shaft power and efficiency. The relation between power and flow coefficients, τ_0 versus ϕ_0, is shown in Fig. 8 (b). The tendency is similar for all impellers,

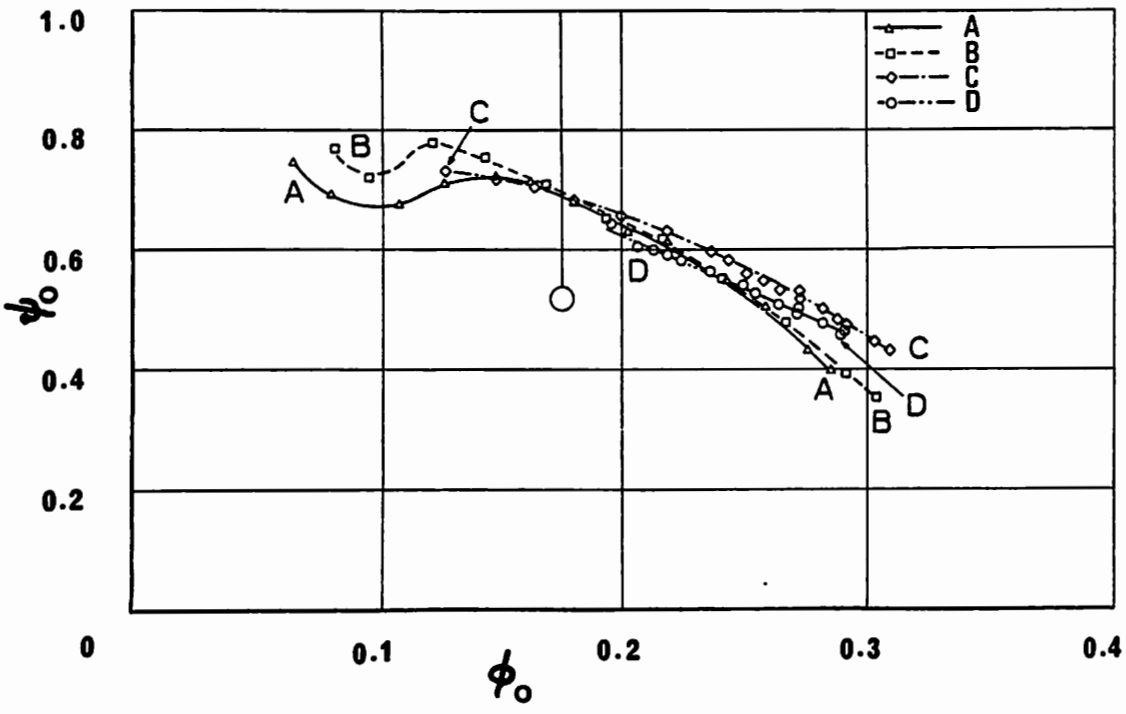

Figure 8. Characteristics referred to the prototype: (a) Pressure rise

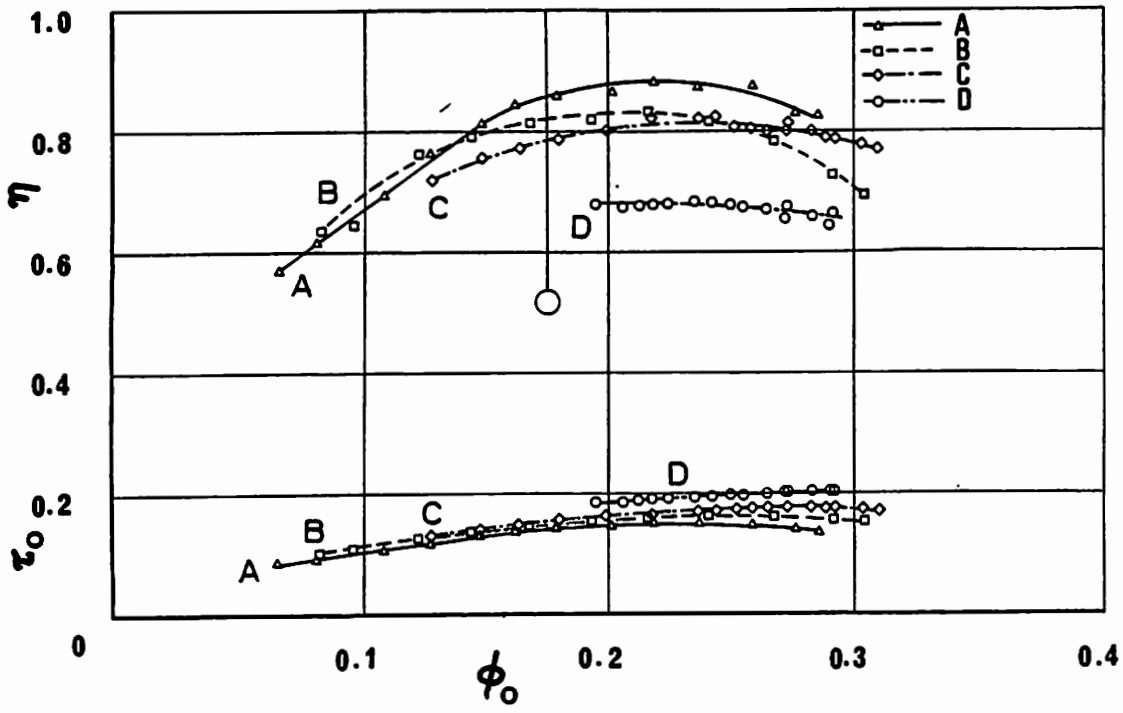

FIGURE 8. Characteristics referred to the prototype:
(b) Input and efficiency

however, the absolute values of power coefficients increase as passage width decreases (Impeller A to D). This is quite understandable, since the losses associated with the wall friction are almost constant independent of passage width but their effect on power consumption or efficiency is relatively larger for an impeller with smaller flow rate.

The efficiency curves can be interpreted by the same understanding. The maximum efficiencies as well as those at design condition are ranked in the order of passage width, Impeller A to D.

Flow rate versus power and efficiency of impeller blades. Power coefficients and efficiencies evaluated by Eq.(3) are plotted against flow coefficient in Fig. 9 for four impellers. As seen from the figure, power coefficients of impeller blades τ_b, excluding the power necessary to rotate hub itself, distribute almost on a single curve for all impellers. At over-flow range, $\phi_0 > 0.25$, small scattering of data becomes evident, where Impeller A has the least power coefficient.

The efficiencies η_b of all impellers coincide beautifully at design condition. The flow coefficient at the maximum efficiency point is different for each impeller and increases as the increase of passage width (Impeller D to A). The maximum efficiencies η_{bmax} are improved also with the passage width from 0.93 of Impeller D to 0.98 of Impeller A.

The behavior of efficiency at off-design condition is not simple as seen from the figure. We may observe a general

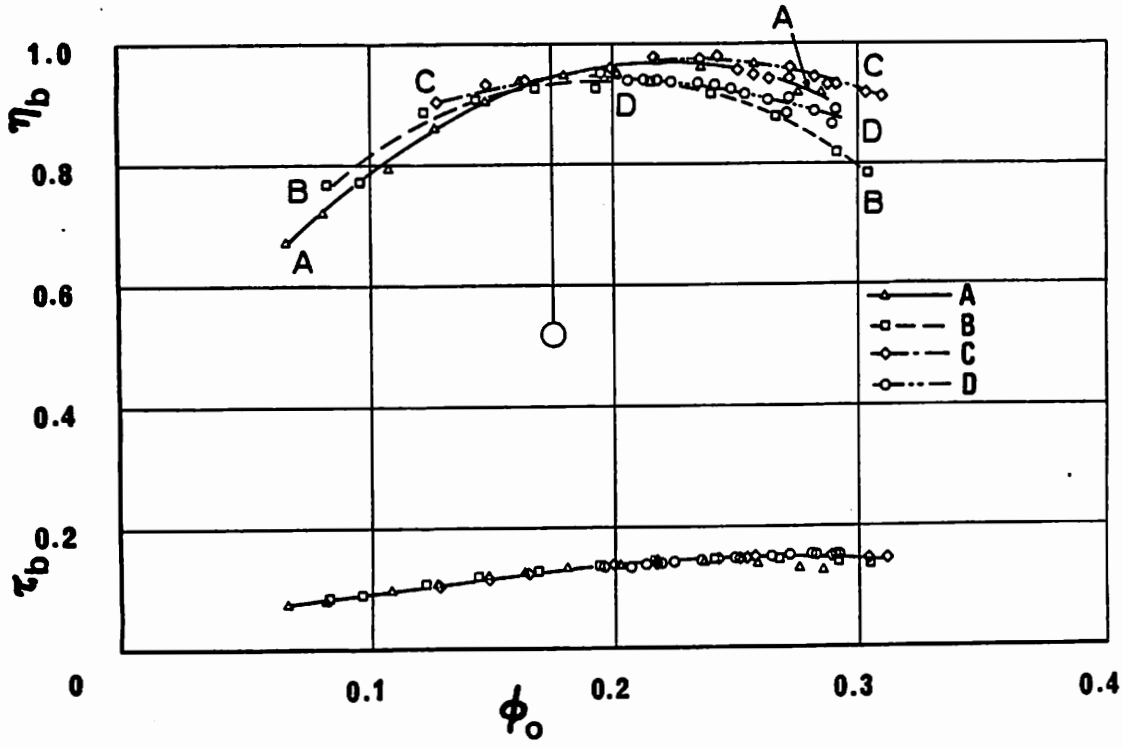

FIGURE 9. Characteristics of impeller blades

tendency that larger efficiency drop takes place at partial flow range in a impeller with wider passage width, while at over-flow range this is not necessarily the case. This may be due to the difference of secondary flow and separation pattern at partial and over-flow range.

The result of Fig. 9 indicates that at least near design condition the characteristics of partial impellers are identical to those of the prototype and hence the real flow in a partial impeller can be considered as a part of the one in the prototype, provided the losses associated with the friction of rotating hub is excluded. Specific speed of a impeller loses its meaning for the interpretation of performance in this case and the design procedure based on quasi-three dimensional analysis proves to be useful for the prediction of performances.

6. CONCLUSION

The result obtained from the performance test of four impellers is summarized as follows.

1. Prototype mixed flow impeller with specific speed of 750 (m^3/min, m, rpm) and its three partial impellers with 3/4, 2/4 and 1/4 design flow rate have almost the same pressure rise coefficient and efficiency near design condition, provided the power necessary to rotate hub is excluded. The efficiencies of all impellers are close to 95 % near design condition;

2. The blade efficiency of a mixed flow impeller remains satisfactorily at a high level at least for the specific speed down to 400 (that of Impeller D). For impellers with specific speed between 400 and 750, the impeller losses can be calculated as the sum of loss in blade passages and a constant loss due to the hub and casing wall friction independent of passage width;
3. The quasi-three dimensional analysis proves to be useful for the prediction of flow and performance of impeller blades near the design condition;
4. At a partial flow rate, an impeller with wider passage width, in which the restriction to three dimensional deflection is weaker, tends to stall and lose pressure rise earlier with flow rate. In other words, the partial flow performance is affected by specific speed.

This study was supported by JSME as a joint research project. The authors are indebted to the project research committee (RC-60, chairman, Prof. T. Ikui) for the advice and incentives.

NOMENCLATURE

D = outer diameter of prototype impeller
d = outer diameter of each impeller
i = multiplication factor
k = type number
L = power
n_s = specific speed
n = rotational speed
ΔP_t = total pressure rise
Q = flow rate
u = peripheral speed
ρ = density
ϕ = flow coefficient
ψ = pressure rise coefficient
τ = power coefficient
η = efficiency

Subscript
0 = normalized by referring to the prototype
b = impeller blade only

REFERENCES

1. Project Research Committee RC-60, Report on Application of Quasi-three Dimensional Analysis to the Design of High Performance Mixed Flow Turbomachinery, JSME, August 1984 (in Japanese).

2. Wiesner, F. J., A Review of Slip Factor for Centrifugal Impellers, Journal of Engineering for Power, Trans. ASME, Ser. A, vol. 89, no. 4, pp. 558-572, 1967.

3. Senoo, Y., and Nakase, Y., A Blade Theory of an Impeller With an Arbitrary Surface of Revolution, Journal of Engineering for Power, Trans. ASME, Ser. A, vol. 93, no. 4, pp. 454-460, 1971.

4. Senoo, Y., and Nakase, Y., An Analysis of Flow Through a Mixed Flow Impellers, Journal of Engineering for Power, Trans. ASME, Ser. A, vol.94, no. 1, pp. 43-50, 1972.